RESEARCH ARTICLE

Interdecadal relationship between the wintertime haze frequency over Beijing and mega-ENSO

Jing Wang[1] | Yanju Liu[2] | Yihui Ding[2]

[1]Key Laboratory of Meteorological Disaster, Ministry of Education (KLME)/Joint International Research Laboratory of Climate and Environment Change (ILCEC)/Collaborative Innovation Center on Forecast and Evaluation of Meteorological Disasters (CIC-FEMD), Nanjing University of Information Science and Technology, Nanjing, China

[2]National Climate Center, China Meteorological Administration, Beijing, China

Correspondence
Yanju Liu, National Climate Center, China Meteorological Administration, Beijing 100081, China.
Email: liuyanj@cma.gov.cn

Abstract

Observational analyses suggest that natural or internal climate variability plays a crucial role in modulating wintertime haze days in Beijing (WHD_{BJ}) on decadal timescales, which may overwhelm the effect of human emissions to some extent. This study links the variations in WHD_{BJ} to the mega-El Niño–Southern Oscillation (ENSO), a newly defined ENSO-related pattern with a vaster range of variability, on decadal timescales. The mega-ENSO delineates an apparent out-of-phase relationship with WHD_{BJ}, which could be used to explain past and recent decreases in WHD_{BJ} in 1961–1971 and 1997–2012, as well as the increase in WHD_{BJ} in 1972–1996. The positive phase of the mega-ENSO can induce a high dynamical scavenging efficiency of pollutants over the Beijing area through notable in situ low-level northerly wind anomalies that are associated with a quasi-barotropic anticyclonic anomaly centered around Lake Baikal, thus reducing the frequency of haze days on decadal time-scales, and vice versa for the negative phase. The mega-ENSO can influence interdecadal predictions of the long-term occurrence of haze events over Beijing. Therefore, it will be focused upon in future routine operations.

KEYWORDS

Beijing, interdecadal variations, mega-ENSO, winter haze frequency

1 | INTRODUCTION

Beijing is the capital of China, possessing a political and economic status of the first magnitude in the country. Beijing city is a haze-prone region (e.g., Cai et al., 2017; Pei et al., 2018). Haze episodes are generally accompanied by fine particulate air pollution (e.g., Ding et al., 2009; Zhang, 2017; An et al., 2019), which can significantly influence the number of deaths induced by cardiovascular and respiratory diseases (Liu et al., 2019). Accordingly, the central government has attached great importance to haze pollution over Beijing and its adjoining areas, implementing efficacious actions [e.g., the "Ten Statements of Atmosphere" (The State Council of the People's Republic of China, 2013) and the "Three-Year Action Plan for Winning the Blue Sky Defense Battle" (The State Council of the People's Republic of China, 2018)] to alleviate in situ hazy conditions.

Because the haze frequency over Beijing and other subregions in central and eastern China (CEC) is highest in the boreal winter (e.g., Mao *et al.*, 2019), the majority of previous studies focused on in situ haze variations in winter. There is a general consensus of opinion on the haze variabilities: winter haze frequency can be significantly modulated by both external anthropogenic emissions (e.g., Yang *et al.*, 2016; Pei *et al.*, 2020) and internal climate anomalies such as atmospheric circulation and El Niño–Southern Oscillation (ENSO) (e.g., Zhang *et al.*, 2014; Wang and Chen, 2016; Ding *et al.*, 2017; Wu *et al.*, 2017; Cheng *et al.*, 2019; Mao *et al.*, 2019; Chang *et al.*, 2020; Wang *et al.*, 2020a, 2020b). It is especially noteworthy that, compared to studies on the interannual variability of winter haze frequency over CEC, studies examining interdecadal timescales are much fewer. The majority of these studies concentrated on the Yangtze River Delta region and the larger domain of CEC, identifying the important roles of interdecadal atmospheric circulation anomalies (Xu *et al.*, 2017) and sea surface temperature (SST) anomalies (SSTAs) such as Pacific Decadal Oscillation (PDO) and Atlantic Multidecadal Oscillation (AMO) (Xiao *et al.*, 2015; Zhao *et al.*, 2016). It is noteworthy that the wintertime haze days in Beijing (WHD$_{BJ}$) also exhibit salient interdecadal variations (Wang *et al.*, 2020b). Nevertheless, it is still not well understood whether the natural interdecadal variability or the anthropogenic influence plays a more vital role in regulating the interdecadal variations of WHD$_{BJ}$.

In this manuscript, we examine if the newly proposed ENSO-related paradigm (viz., mega-ENSO; Wang *et al.*, 2013) can play a more significant role in modulating WHD$_{BJ}$ on interdecadal timescales. Mega-ENSO is defined as the SST difference between the western Pacific (WP) K-shape region and the eastern Pacific (EP) triangle-shape region, which is related to but distinct from the traditional ENSO on interannual timescales; and while on decadal timescales, mega-ENSO mainly reflects the variability of PDO/Interdecadal Pacific Oscillation (IPO) (Wang *et al.*, 2013; Sun *et al.*, 2020). Although the notion of mega-ENSO was originally proposed to investigate summer monsoon variability in the northern hemisphere (Wang *et al.*, 2013), wintertime mega-ENSO can also exert profound impacts on concurrent large-scale climate anomalies by stimulating teleconnections (Wu and Zhang, 2015; Zhang *et al.*, 2017, 2019a, 2019b). Furthermore, mega-ENSO features a broader range of spatiotemporal variability than ENSO, PDO, and IPO alone (Wang *et al.*, 2013) and the prominent zonal SST gradient between the WP region and the EP region (Zhan *et al.*, 2017) on multitimescales. The above features may not be reflected by other SST modes in the Pacific Ocean such as PDO and IPO

(Newman *et al.*, 2016; Zhang *et al.*, 2018; Huang *et al.*, 2019), although they have a resembled spatial pattern as mega-ENSO (Wang *et al.*, 2013). Consequently, we selected mega-ENSO instead of PDO/IPO in this study. This work may help the Chinese government formulate long-term anthropogenic emissions planning to address the wintertime hazy conditions over Beijing area.

2 | DATA AND METHODS

The datasets used in this study comprise (a) ground-timing observation datasets four times per day at 02:00, 08:00, 14:00, and 20:00 (Beijing local time) for 1961–2019, from the National Meteorological Information Center of China (http://data.cma.cn/); (b) monthly planetary boundary layer height (PBLH) for 1979–2019 from the European Centre for Medium-Range Weather Forecasts Interim Reanalysis (ERA-Interim) (Dee *et al.*, 2011); (c) monthly atmospheric data for 1961–2019 from the National Centers for Environmental Prediction (NCEP)–National Center for Atmospheric Research (NCAR) Reanalysis I (NCEP/NCAR) (Kalnay *et al.*, 1996); (d) monthly Extended Reconstructed SST dataset version 5 (ERSST v5) for 1961–2019 from the National Oceanic and Atmospheric Administration (NOAA) (Huang *et al.*, 2017); and (e) annual total energy consumption in the Jing-Jin-Ji region for 1986–2016 from the National Bureau of Statistics of China (http://www.stats.gov.cn/).

In this study, we selected the national reference climatological station (station name: Beijing; station number: 54511) to study the interdecadal haze changes in Beijing, which is fairly representative of the entire Beijing area over longer observation periods (Zheng *et al.*, 2019). The definition of a haze day is consistent with those of the previous studies (Chen and Wang, 2015; Wang *et al.*, 2018, 2019). To be specific, a haze day in Beijing is deemed to have occurred when the corresponding surface observations of relative humidity, visibility and wind speed satisfy the following criteria once among the four times per day: visibility lower than 10 km (7.66 km since the year 2013; Pei *et al.*, 2018), relative humidity lower than 90%, and the surface wind speed lower than 7 m·s^{-1}. Further, recent studies (e.g., Li *et al.*, 2020) noted that an abrupt decrease in relative humidity could be detected around the early 2000s, when an automatic observation system was implemented in China. However, the automatic observations of relative humidity over the regions north of the Yangtze River in winter were relatively less affected (e.g., Wang *et al.*, 2007), so they could not exert tangible impact on the consistency of time series data on haze days before and after the early 2000s.

In addition, we employed ERSST v5 data to construct the monthly mega-ENSO index, which is defined by using the mean WP K-shape SST minus the mean EP triangle-shape SST (Figure 2a), and the SSTA patterns regressed against the summer and winter mega-ENSO index in this study (not shown) agree with those of previous studies (Wang *et al.*, 2013; Wu and Zhang, 2015). Note that the positive phase of mega-ENSO is characterized by SST warming in the WP K-shape region together with SST cooling in the EP triangle-shape region and vice versa, and mega-ENSO accounts for approximately 18.0% of the total variance of SSTA in the Pacific (Wang *et al.*, 2013).

Throughout this manuscript, we focus on the boreal winter (December–February; DJF). To remove the possible influences of the long-term trends in variables, all data were linearly detrended before analyses. We deployed a low-pass filter using the 11-year running mean to extract the interdecadal component with a 10-year cutoff period for the filtered variables. The two-tailed Student's *t* test was used to evaluate the statistical significance. The wave activity flux (WAF; Takaya and Nakamura, 2001) was used to indicate the tendency of Rossby wave energy propagation.

Similar to the approach of Zhan *et al.* (2017), we utilized an atmospheric general circulation model (AGCM), the fifth generation Max Planck Institute model in Hamburg (ECHAM5) (Roeckner *et al.*, 2003), to confirm our proposed mechanisms. The resolution of the model is T42 and 19 vertical levels. Two numerical experiments, a control run and a sensitivity run, were performed. The control experiment was integrated for 30 years with a prescribed climatological monthly mean SST, and the last 20 year means during DJF were analyzed. In the sensitivity experiment concerning mega-ENSO, the model was performed in a similar manner but forced by the imposed climatological SST plus SSTAs in the Pacific between 40°S and 40°N, as shown in Figure 2a. Thus, the differences between the sensitivity experiment and the control experiment can determine the impacts of mega-ENSO.

3 | RESULTS

Figure 1 illustrates the time series of the anomalous original WHD_{BJ} as well as the detrended WHD_{BJ} and its corresponding 11-year running average during 1961–2018. The detrended WHD_{BJ} can explain 95.9% of the total variance of the original WHD_{BJ}. Moreover, the time series of WHD_{BJ} clearly exhibits interdecadal fluctuations (bars). Three abrupt interdecadal changes in the evolution of WHD_{BJ} can be detected, specifically around the early 1970s (shift from negative to positive values), after the mid-1990s (shift from positive to negative) and after the early-2010s (shift from negative to positive). As such, the entire period can be primarily divided into four epochs: pre-P1 (1961–1971), P1 (1972–1996), P2 (1997–2012), and post-P2 (2013–2018). It is noteworthy that although there is a sharp increase in the total energy consumption in and around Beijing during P2 compared to that during P1 (Figure 3), WHD_{BJ} is lower than normal in P2 whereas there is more haze occurrence in P1. Consequently, it is plausible to speculate that the internal interdecadal climate variability should play a more
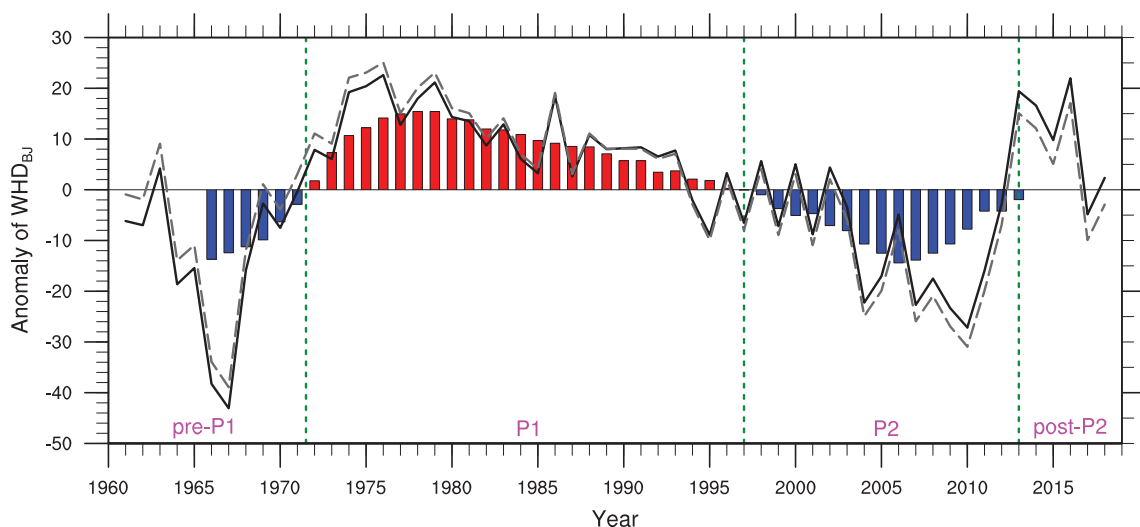
FIGURE 1 Time series of the anomalies in raw WHD_{BJ} (dashed curve, days) as well as detrended WHD_{BJ} (solid curve, days) and its corresponding 11-year running average (bars, days) during 1961–2018. Vertical lines delineate transition periods for the running average. "pre-P1", "P1", "P2", and "post-P2" denote the subperiods of 1961–1971, 1972–1996, 1997–2012, and 2013–2018, respectively

critical role in modulating the interdecadal WHD$_{BJ}$ variability.

As shown in Figure 2a, the DJF composite difference map of SST between P1 and P2 delineates, overall, a conspicuous zonal dipolar pattern with SST warming (cooling) in the K-shape (triangle-shape) region with obvious trade wind anomalies, which is similar to the positive phase of the mega-ENSO pattern (or mega-La Niña) (Zhang *et al.*, 2019b, their Figure 3a). We further examined the Pacific SSTA patterns by showing the differences between pre-P1 and P1 as well as between P2 and post-P2 (Figure S1). Similar and stable Pacific SSTA patterns could clearly be found, which implies that the Pacific SST may play an important role in the modulation of the interdecadal variability of winter haze occurrence frequency in Beijing, although there was a lower level of total energy consumption in pre-P1. Consequently, it is proposed that the recent diminution in haze occurrence in P2 could be well interpreted from the transition of mega-ENSO from the negative to the positive phase. The
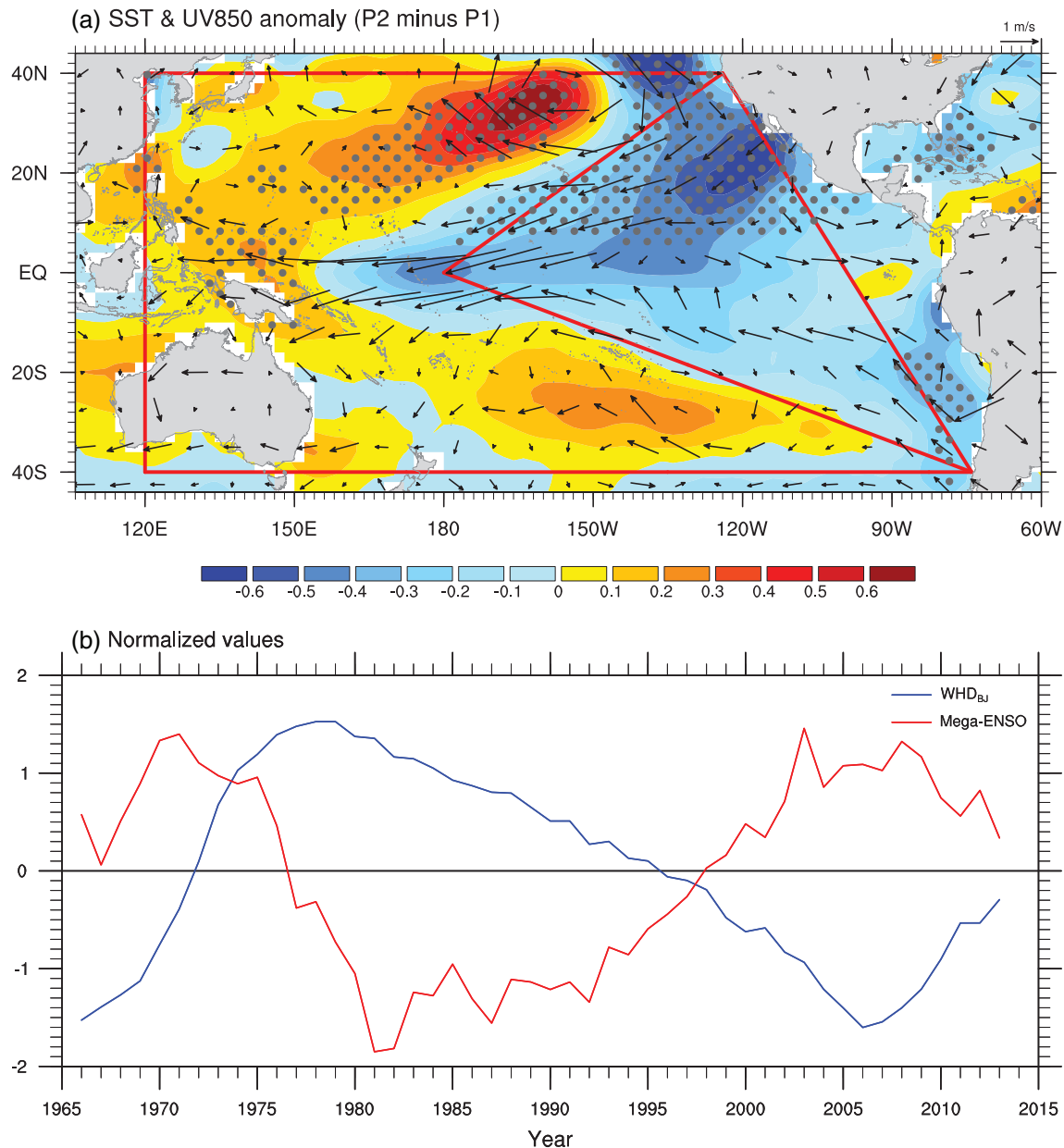
FIGURE 2 (a) DJF composite differences of SST (shaded, °C) and 850-hPa winds (vectors, m·s^{-1}) during the period between P1 (1972–1996) and P2 (1997–2012) (P2 minus P1) after removing the linear trend. The stippled areas indicate values of SSTAs exceeding the 90% confidence level. (b) Time series of the normalized 11-year low-pass-filtered anomalous WHD$_{BJ}$ (blue curve) and the concurrent mega-ENSO index (red curve) from 1966 to 2013 after removing the linear trend. The red lines in panel (a) show the western Pacific K-shape and the eastern Pacific triangle-shape regions, which are deployed in defining the mega-ENSO index according to Wang *et al.* (2013)

Energy consumption in Jing-Jin-Ji region (1986-2016)
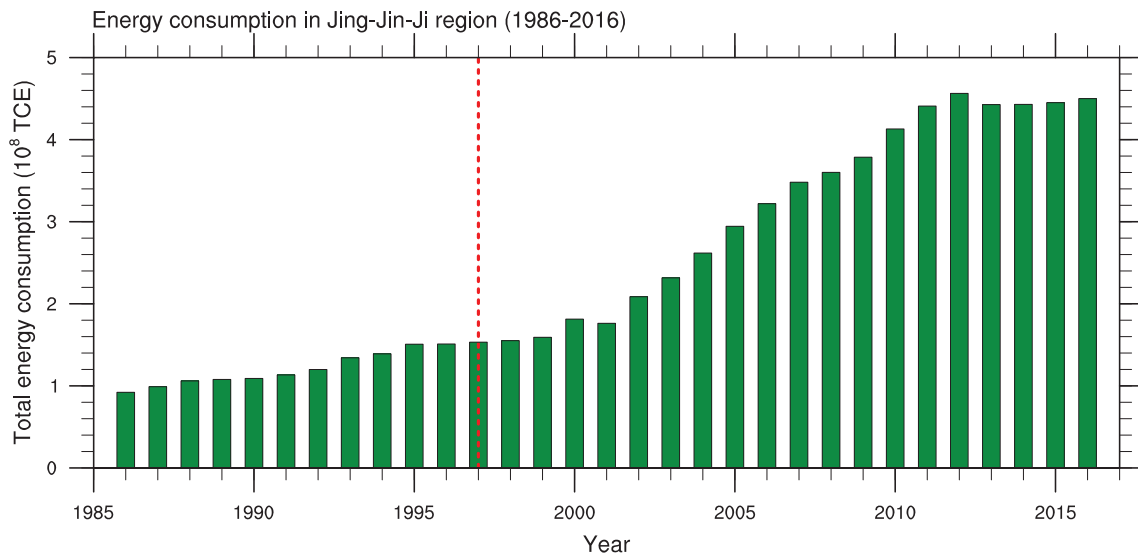
FIGURE 3   Time series of the total energy consumption (green bars, 10^8 TCE) in the Jing-Jin-Ji region during 1986–2016. The red vertical line indicates the year 1997

aforementioned mega-ENSO–WHD$_{BJ}$ relationship on decadal timescales can be clearly observed in Figure 2b. Fluctuations in the normalized WHD$_{BJ}$ appear to be out of phase with those in the concurrent mega-ENSO index.

A question arises here pertaining to how mega-ENSO influences the WHD$_{BJ}$ on decadal timescales. Before addressing this, the anomalies of boundary layer parameters tied to the winter haze variability in Beijing should be revisited. A higher WHD$_{BJ}$ is associated with significantly warmer and moister surface conditions (Figure S2a,b) as well as the stable atmospheric stratification at lower levels (Figure S2f), in conjunction with decreased surface wind, sea-level pressure (SLP), PBLH, and surface southerly wind anomalies deduced from the spatial distribution of SLP anomalies (Figure S2c–e), which is in line with previous studies (Yin *et al.*, 2017; Wang *et al.*, 2020a). In fact, these anomalous boundary conditions are indicative of conducive environmental circumstances, favoring the transportation and accumulation of in situ aerosols and water vapor over Beijing and its surroundings. As such, the positive localized feedback loop effect between aerosols and meteorology can be triggered (Li *et al.*, 2017; An *et al.*, 2019), which may boost the in situ haze frequency.

Next, we present some explanations regarding the possible impacts of mega-ENSO. Figure 4 shows the DJF composite differences of geopotential height and wind between P1 and P2 (P2 minus P1). Corresponding to the mega-La Niña, there is a quasi-barotropic 500-hPa (Figure 4a) and 850-hPa (Figure 4b) anticyclonic anomaly centered around Lake Baikal, indicating a southward shift of Mongolian High (Figure 5d) with noticeable low-level northeasterly/northerly wind anomalies controlling

the Beijing area, which is somewhat similar to the climatological conditions (Figure S3). Under the influence of this anticyclonic anomaly, the atmosphere can effectively diffuse the amassed near-surface pollutants and water vapor over Beijing via the intensified surface northerly winds around Beijing along the eastern flank of Mongolian High (Figure 5c,d), suggesting the dampened localized air stagnation. Accordingly, the low-level air around Beijing is significantly unstable (Figure 5f), which can generally increase the PBLH around Beijing although some weak negative PBLH anomalies exist (Figure 5e). Because the consistent anticyclonic anomaly lies more southward (Figures 4 and 5d), it may hinder intrusion of high latitude cold air with quite dry and pristine conditions into North China. As such, the associated northerly wind anomalies cannot sufficiently decrease the temperature and relative humidity over Beijing, which may cause weak in situ surface temperature and moisture anomalies (Figure 5a,b). It should be pointed out that such positive temperature anomalies may signify a weak response of the East Asian winter monsoon to the mega-ENSO (Zhang *et al.*, 2019b). Under the above environmental circumstances, despite the fact that localized positive temperature and relative humidity anomalies can facilitate the formation of secondary aerosols (Jacob and Winner, 2009; Ding and Liu, 2014; Tie *et al.*, 2017), the stronger-than-normal dynamical dispersion of pollutants associated with the in situ marked northerlies during the positive phase of mega-ENSO could play a decisive role in the lower WHD$_{BJ}$ on decadal timescales. Furthermore, because pre-P1 corresponds to the positive phase of mega-ENSO (Figures 1 and 2b), we can infer that the mega-La Niña may also contribute to a decreased WHD$_{BJ}$
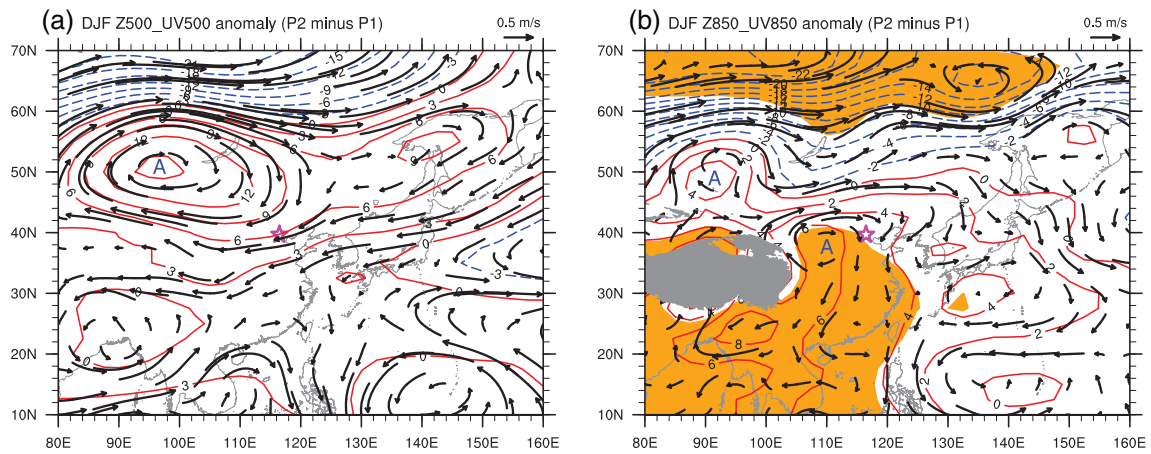
FIGURE 4 DJF composite differences of geopotential height (contours, gpm) and wind (vectors, m·s⁻¹) during the period between P1 (1972–1996) and P2 (1997–2012) (P2 minus P1) after removing the linear trend at (a) 500 hPa and (b) 850 hPa. Values of geopotential height anomalies that are significant at the 90% confidence level are shaded. The pentagram delineates the location of Beijing, and the gray shaded area denotes the Tibetan plateau. The letter a represents the center of anomalous anticyclonic circulation
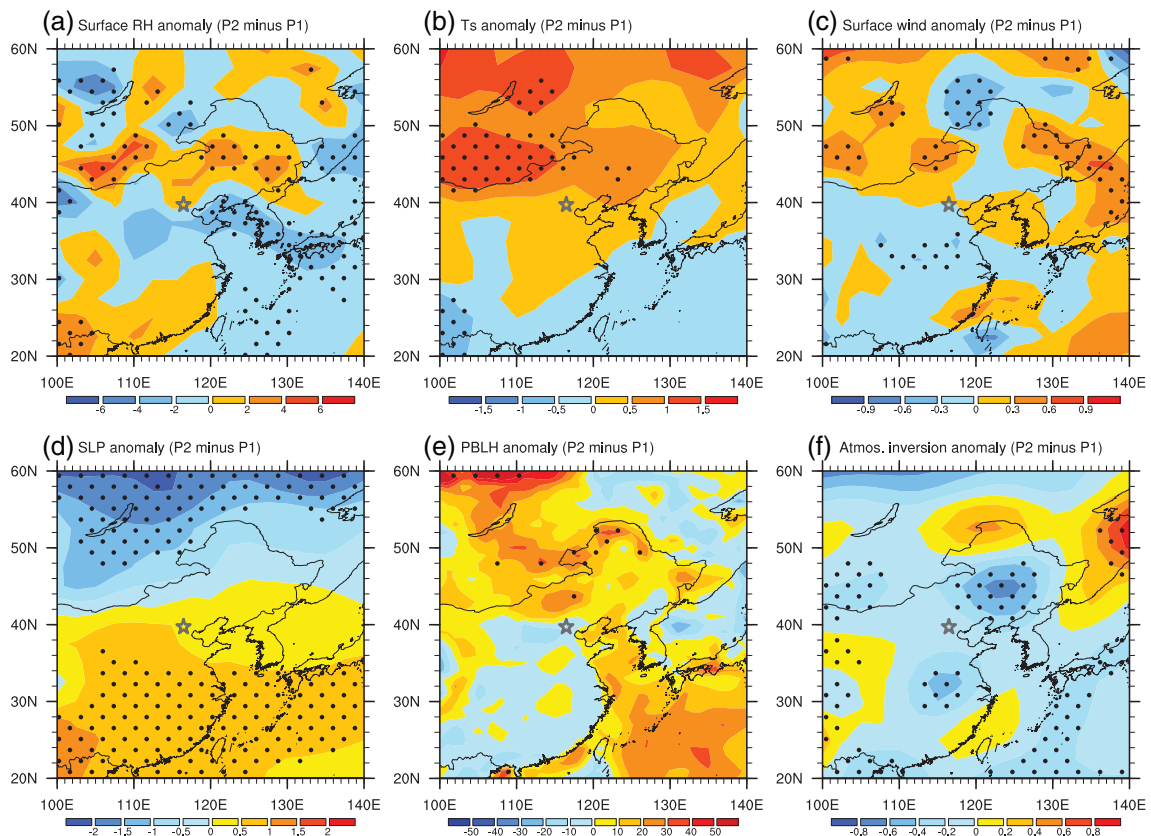
FIGURE 5 (a) DJF composite differences of surface relative humidity (shaded, %), (b) surface air temperature (shaded, °C), (c) surface wind speed (shaded, m·s⁻¹), (d) SLP (shaded, hPa), (e) PBLH (shaded, m), and (f) air temperature between 850 and 1,000 hPa (shaded, °C) during the period between P1 (1972–1996) and P2 (1997–2012) (P2 minus P1) after removing the linear trend. Values that are significant at the 90% confidence level are stippled. The pentagram delineates the location of Beijing

during pre-P1 considering the connected meteorological anomalies (Figure S4). Similarly, the negative phase of mega-ENSO (i.e., mega-El Niño) (Zhang *et al*., 2019a) could be responsible for the enhancement of WHD$_{BJ}$ during P1.

4 | CONCLUSIONS AND DISCUSSION

The climate variability of natural or internal nature on decadal timescales could play a more considerable role in modulating winter haze variability over Beijing compared to anthropogenic emissions, which is consistent with the findings of previous studies (e.g., Pei *et al*., 2020). Our observational analyses suggest that, on interdecadal timescales, there is a noticeable out-of-phase relationship between WHD$_{BJ}$ and DJF mega-ENSO, which may be responsible for the decrease in WHD$_{BJ}$ in recent and prior subperiods P2 (1997–2012) and pre-P1 (1961–1971), as well as the increase in WHD$_{BJ}$ in subperiod P1 (1972–1996). The quasi-barotropic anticyclonic anomaly centered around Lake Baikal, which is associated with the mega-La Niña (the positive phase of mega-ENSO), can enhance the dynamical diffusion efficiency of near-surface pollutants over Beijing through enhanced low-level consistent northerly wind anomalies, increasing the number of epochal WHD$_{BJ}$; and vice versa for the negative phase.

Furthermore, the following four central points, which deserve further discussion, are especially noteworthy. First, distinctive circulation anomalies over the extratropical areas in winter can be triggered by disparate ENSO flavors such as traditional equatorial ENSO and new-defined mega-ENSO (e.g., Weng *et al*., 2009; Yuan and Yang, 2012; Zhang *et al*., 2015; Zhang *et al*., 2019a, 2019b; Hu *et al*., 2020). However, here we unravel that the mega-ENSO mode plays a more pivotal role in

modulation. For instance, as investigated above, the mega-La Niña events could be responsible for fewer WHD$_{BJ}$ in P2. Nonetheless, we can discern that the significant SST cooling/warming are confined over the extratropical EP/WP Pacific sector in the northern hemisphere instead of the equatorial oceanic regions (Figure 2a), suggesting that the extratropical SSTAs tied to mega-La Niña have a more crucial role than those connected to the conventional equatorial La Niña. The most significant difference between mega-La Niña and conventional La Niña is that the former features vaster banded negative SSTAs over the extratropical EP sector as well as positive SSTAs over the WP sector in both hemispheres. Although the obvious negative SSTAs are mainly located in the equatorial oceanic regions during pre-P1, the remarkable positive SSTAs are located in the WP extratropical oceans, also indicating the potential appreciable role of mega-La Niña (Figure S1a).

Second, the physics of how mega-ENSO regulates the anticyclonic/cyclonic anomaly centered around Lake Baikal should be examined. In fact, while specifically aiming at the mega-ENSO on decadal timescales from the perspective of global circulation anomalies (Figure 6), we can clearly detect a marked quasi-barotropic planetary-scale zonal Rossby wavetrain with alternating cyclonic and anticyclonic anomalies, which can transmit the influence of remote mega-ENSO events to North China through such a far-reaching zonal teleconnection. Consequently, positive mega-ENSO is associated with anomalously enhanced geopotential height in the middle troposphere over Northeast Asia (Figure 6), leading to prominent downward motions over Lake Baikal (Figure S5) and in turn inducing the in situ anticyclonic anomaly. As a matter of fact, the DJF mega-ENSO can excite the poleward-propagating Rossby wave (Zhang *et al*., 2019a), and the westerly jet stream (WJS) often serves as the waveguide facilitating the Rossby wave energy propagation into the downstream areas
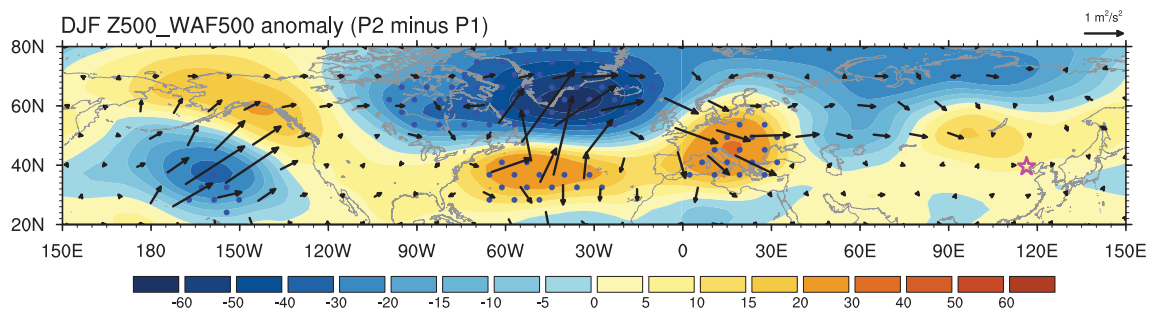
FIGURE 6 DJF composite differences of 500-hPa geopotential height (contours, gpm) and WAF (vectors, m^2·s^{-2}) during the period between P1 (1972–1996) and P2 (1997–2012) (P2 minus P1) after removing the linear trend. Values of geopotential height anomalies that are significant at the 90% confidence level are dotted. The pentagram delineates the location of Beijing
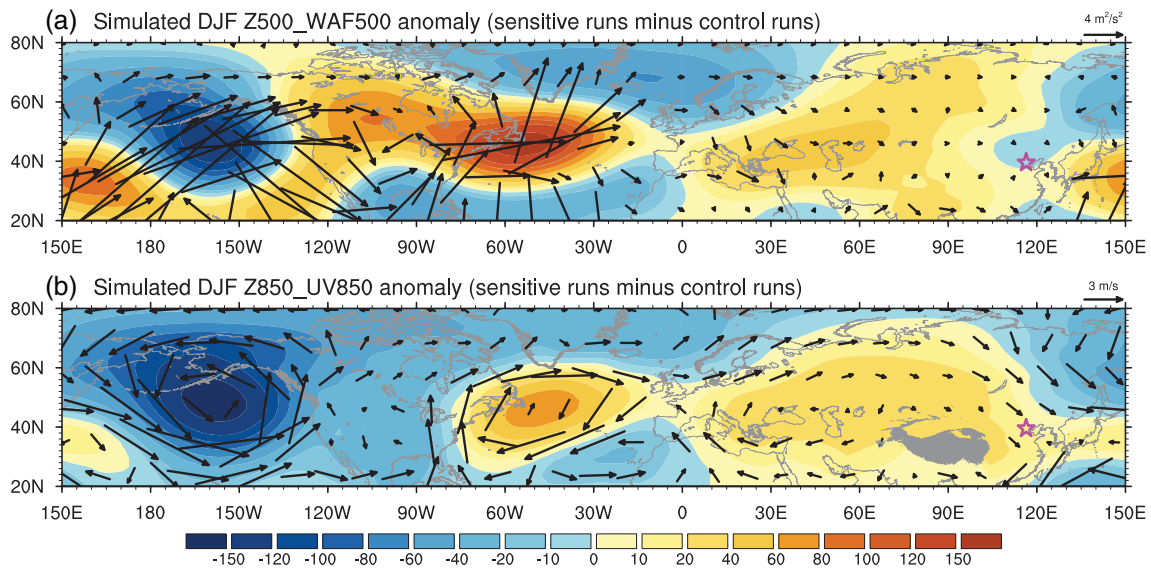
FIGURE 7 Simulated DJF differences of (a) 500-hPa geopotential height (contours, gpm) and WAF (vectors, $m^2 \cdot s^{-2}$) and (b) 850-hPa geopotential height (contours, gpm) and 850-hPa wind (vectors, $m \cdot s^{-1}$) between the sensitive run and the control run based on the ECHAM model. The pentagram delineates the location of Beijing, and the gray shaded area denotes the Tibetan plateau

(e.g., Ambrizzi and Hoskins, 1997; Zhang *et al.*, 2015; Zhu and Li, 2016; Wang *et al.*, 2019). We assume that the poleward-propagating Rossby wave might be trapped when it passes across the WJS. Subsequently, under the influence of the WJS waveguide, the above planetary-scale zonal wavetrain with significant perturbations might affect the interdecadal variability of the downstream wintertime anticyclonic anomaly centered around Lake Baikal. The above-mentioned processes and wave path can be supported by the composite maps of stationary WAF (vectors in Figure 6). To further validate the proposed physical processes/mechanisms, numerical experiments associated with mega-ENSO were performed. The observed quasi-barotropic teleconnection and WAFs associated with the positive mega-ENSO can be reproduced using the ECHAM5 model overall, with much broader positive height anomalies over northern Asia (Figure 7a). Therefore, noticeable modeled low-level northerly wind anomalies over Beijing can be triggered (Figure 7b) to establish a higher dynamical scavenging efficiency of local pollutants.

Third, we find that the spatial SSTA distribution in the years after P2 (2013–2018) exhibits a somewhat mega-El Niño-like pattern (Figure S6). Whether the increased mean higher number of WHD_{BJ} after 2013 (Figure 1) are associated with the mega-El Niño episodes is an intriguing issue that deserves further exploration.

Fourth, it was observed that DJF AMO exhibits clear interdecadal fluctuations around the early 1970s (switching from positive to negative) and mid-1990s

(switching from negative to positive) (Geng *et al.*, 2017), and it has a fairly similar in-phase interdecadal relationship with mega-ENSO. As revealed by previous studies (Xiao *et al.*, 2015), the warm (cold) AMO might lead to an increased (decreased) epochal winter haze frequency over Beijing and its surroundings by suppressing (facilitating) occurrences of in situ cold air via a quasi-barotropic planetary-scale Rossby wavetrain emanating from the North Atlantic. However, the actual decreased epochal WHD_{BJ} during P2 (corresponding to warm AMO) and increased epochal WHD_{BJ} during P1 (corresponding to cold AMO) allow us to speculate that AMO could play a relatively minor role in modulating WHD_{BJ} on decadal timescales compared to mega-ENSO. Furthermore, it was found that AMO can modulate variations in PDO/IPO on decadal timescales through atmospheric bridge**s** (Si and Ding, 2016; Kosaka, 2018; Zhang *et al.*, 2018). Therefore, the existence of appreciable interactions between DJF AMO and mega-ENSO, if any, should be ascertained. These issues are deserving of further investigations in future studies.

ORCID

Jing Wang https://orcid.org/0000-0002-6293-6176
Yanju Liu https://orcid.org/0000-0003-1462-743X
Yihui Ding https://orcid.org/0000-0001-6246-8897

REFERENCES

Ambrizzi, T. and Hoskins, B.J. (1997) Stationary Rossby-wave propagation in a baroclinic atmosphere. *Quarterly Journal of the Royal Meteorological Society*, 123(540), 919–928.

An, Z., Huang, R.-J., Zhang, R., Tie, X., Li, G., Cao, J., Zhou, W., Shi, Z., Han, Y., Gu, Z. and Ji, Y. (2019) Severe haze in northern China: a synergy of anthropogenic emissions and atmospheric processes. *Proceedings of the National Academy of Sciences of the United States of America*, 116(18), 8657–8666.

Cai, W.J., Li, K., Liao, H., Wang, H.J. and Wu, L.X. (2017) Weather conditions conducive to Beijing severe haze more frequent under climate change. *Nature Climate Change*, 7(4), 257–262.

Chang, Y., Wang, J., Zhu, Z., Deng, H., He, J. and Lu, R. (2020) A salient oceanic driver for the interannual variability of wintertime haze days over the Pearl River Delta region, China. *Theoretical and Applied Climatology*, 140(1), 739–750.

Chen, H.P. and Wang, H.J. (2015) Haze days in North China and the associated atmospheric circulations based on daily visibility data from 1960 to 2012. *Journal of Geophysical Research: Atmospheres*, 120(12), 5895–5909.

Cheng, X., Boiyo, R., Zhao, T., Xu, X., Gong, S., Xie, X. and Shang, K. (2019) Climate modulation of Niño3.4 SST-anomalies on air quality change in southern China: application to seasonal forecast of haze pollution. *Atmospheric Research*, 225, 157–164.

Dee, D.P., Uppala, S.M., Simmons, A.J., Berrisford, P., Poli, P., Kobayashi, S., Andrae, U., Balmaseda, M.A., Balsamo, G., Bauer, P., Bechtold, P., Beljaars, A.C.M., van de Berg, L., Bidlot, J., Bormann, N., Delsol, C., Dragani, R., Fuentes, M., Geer, A.J., Haimberger, L., Healy, S.B., Hersbach, H., Hólm, E. V., Isaksen, L., Kållberg, P., Köhler, M., Matricardi, M., McNally, A.P., Monge-Sanz, B.M., Morcrette, J.J., Park, B.K., Peubey, C., de Rosnay, P., Tavolato, C., Thépaut, J.N. and Vitart, F. (2011) The ERA-interim reanalysis: configuration and performance of the data assimilation system. *Quarterly Journal of the Royal Meteorological Society*, 137, 553–597.

Ding, Y.H., Li, Q.P., Liu, Y.J., Zhang, L., Song, Y.F. and Zhang, J. (2009) Atmospheric aerosols, air pollution and climate change (in Chinese). *Meteorological Monthly*, 35(3), 3–15.

Ding, Y.H. and Liu, Y.J. (2014) Analysis of long-term variations of fog and haze in China in recent 50 years and their relations with atmospheric humidity. *Science China Earth Sciences*, 57 (1), 36–46.

Ding, Y.H., Wu, P., Liu, Y.J. and Song, Y.F. (2017) Environmental and dynamic conditions for the occurrence of persistent haze events in North China. *Engineering*, 3(2), 266–271.

Geng, X., Zhang, W., Stuecker, M.F., Liu, P., Jin, F.-F. and Tan, G. (2017) Decadal modulation of the ENSO–east Asian winter monsoon relationship by the Atlantic multidecadal oscillation. *Climate Dynamics*, 49(7), 2531–2544.

Hu, S., Zhang, W., Turner, A.G. and Sun, J. (2020) How does El Niño-southern oscillation affect winter fog frequency over eastern China? *Climate Dynamics*, 54(1), 1043–1056.

Huang, B.Y., Thorne, P.W., Banzon, V.F., Boyer, T., Chepurin, G., Lawrimore, J.H., Menne, M.J., Smith, T.M., Vose, R.S. and Zhang, H.M. (2017) Extended Reconstructed Sea surface temperature, version 5 (ERSSTv5): upgrades, validations, and intercomparisons. *Journal of Climate*, 30(20), 8179–8205.

Huang, Y., Wu, B., Li, T., Zhou, T. and Liu, B. (2019) Interdecadal Indian Ocean basin mode driven by Interdecadal Pacific oscillation: a season-dependent growth mechanism. *Journal of Climate*, 32(7), 2057–2073.

Jacob, D.J. and Winner, D.A. (2009) Effect of climate change on air quality. *Atmospheric Environment*, 43(1), 51–63.

Kalnay, E., Kanamitsu, M., Kistler, R., Collins, W., Deaven, D., Gandin, L., Iredell, M., Saha, S., White, G., Woollen, J., Zhu, Y., Chelliah, M., Ebisuzaki, W., Higgins, W., Janowiak, J., Mo, K. C., Ropelewski, C., Wang, J., Leetmaa, A., Reynolds, R., Jenne, R. and Joseph, D. (1996) The NCEP/NCAR 40-year reanalysis project. *Bulletin of the American Meteorological Society*, 77(3), 437–471.

Kosaka, Y. (2018) Slow warming and the ocean see-saw. *Nature Geoscience*, 11(1), 12–13.

Li, Z., Guo, J., Ding, A., Liao, H., Liu, J., Sun, Y., Wang, T., Xue, H., Zhang, H. and Zhu, B. (2017) Aerosol and boundary-layer interactions and impact on air quality. *National Science Review*, 4(6), 810–833.

Li, Z., Yan, Z., Zhu, Y., Freychet, N. and Tett, S. (2020) Homogenized daily relative humidity series in China during 1960–2017. *Advances in Atmospheric Sciences*, 37(4), 318–327.

Liu, C., Chen, R., Sera, F., Vicedo-Cabrera, A.M., Guo, Y., Tong, S., Coelho, M.S.Z.S., Saldiva, P.H.N., Lavigne, E., Matus, P., Valdes Ortega, N., Osorio Garcia, S., Pascal, M., Stafoggia, M., Scortichini, M., Hashizume, M., Honda, Y., Hurtado-Díaz, M., Cruz, J., Nunes, B., Teixeira, J.P., Kim, H., Tobias, A., Íñiguez, C., Forsberg, B., Åström, C., Ragettli, M.S., Guo, Y.-L., Chen, B.-Y., Bell, M.L., Wright, C.Y., Scovronick, N., Garland, R.M., Milojevic, A., Kyselý, J., Urban, A., Orru, H., Indermitte, E., Jaakkola, J.J.K., Ryti, N.R.I., Katsouyanni, K., Analitis, A., Zanobetti, A., Schwartz, J., Chen, J., Wu, T., Cohen, A., Gasparrini, A. and Kan, H. (2019) Ambient particulate air pollution and daily mortality in 652 cities. *New England Journal of Medicine*, 381(8), 705–715.

Mao, L., Liu, R., Liao, W., Wang, X., Shao, M., Liu, S.C. and Zhang, Y. (2019) An observation-based perspective of winter haze days in four major polluted regions of China. *National Science Review*, 6(3), 515–523.

Newman, M., Alexander, M.A., Ault, T.R., Cobb, K.M., Deser, C., Di Lorenzo, E., Mantua, N.J., Miller, A.J., Minobe, S., Nakamura, H., Schneider, N., Vimont, D.J., Phillips, A.S., Scott, J.D. and Smith, C.A. (2016) The Pacific decadal oscillation, revisited. *Journal of Climate*, 29(12), 4399–4427.

Pei, L., Yan, Z.W., Sun, Z.B., Miao, S.G. and Yao, Y. (2018) Increasing persistent haze in Beijing: potential impacts of weakening East Asian winter monsoons associated with northwestern Pacific sea surface temperature trends. *Atmospheric Chemistry and Physics*, 18(5), 3173–3183.

Pei, L., Yan, Z., Chen, D. and Miao, S. (2020) Climate variability or anthropogenic emissions: which caused Beijing haze? *Environmental Research Letters*, 15(3), 034004.

Roeckner, E., Bäuml, G., Bonaventura, L., Brokopf, R., Esch, M., Giorgetta, M., Hagemann, S., Kirchner, I., Kornblueh, L., Manzini, E., Rhodin, A., Schlese, U., Schulzweida, U. and Tompkins, A. (2003) *The Atmospheric General Circulation Model ECHAM5: Part I. Max Planck Institute for Meteorology Rep. 349*. Hamburg, Germany: Max Planck Institute for Meteorology, p. 127.

Si, D. and Ding, Y. (2016) Oceanic forcings of the interdecadal variability in east Asian summer rainfall. *Journal of Climate*, 29 (21), 7633–7649.

Sun, Y., Zhong, Z., Li, T., Yi, L., Shi, J., Shen, Y., Liu, K., Hu, Y. and Xu, Z. (2020) Superiority of mega-ENSO index in the seasonal prediction of tropical cyclone activity over the western North Pacific. *Earth and Space Science*, 7(5), e2019EA001009.

Takaya, K. and Nakamura, H. (2001) A formulation of a phase-independent wave-activity flux for stationary and migratory quasigeostrophic eddies on a zonally varying basic flow. *Journal of the Atmospheric Sciences*, 58(6), 608–627.

The State Council of the People's Republic of China. (2013). *Air Pollution Prevention and Control Action Plan*. Beijing, P.R. China: The State Council of the People's Republic of China, (in Chinese). http://www.gov.cn/zwgk/2013-09/12/content_2486773.htm.

The State Council of the People's Republic of China. (2018). *Notice of the State Council on Issuing the Three-Year Action Plan for Winning the Blue Sky Defense Battle*. Beijing, P.R. China: The State Council of the People's Republic of China, (in Chinese). http://www.gov.cn/zhengce/content/2018-07/03/content_5303158.htm.

Tie, X.X., Huang, R.-J., Cao, J.J., Zhang, Q., Cheng, Y.F., Su, H., Chang, D., Pöschl, U., Hoffmann, T., Dusek, U., Li, G.H., Worsnop, D.R. and O'Dowd, C.D. (2017) Severe pollution in China amplified by atmospheric moisture. *Scientific Reports*, 7 (1), 15760.

Wang, B., Liu, J., Kim, H.-J., Webster, P.J., Yim, S.-Y. and Xiang, B. (2013) Northern hemisphere summer monsoon intensified by mega-El Niño/southern oscillation and Atlantic multidecadal oscillation. *Proceedings of the National Academy of Sciences of the United States of America*, 110(14), 5347–5352.

Wang, H.J. and Chen, H.P. (2016) Understanding the recent trend of haze pollution in eastern China: roles of climate change. *Atmospheric Chemistry and Physics*, 16(6), 4205–4211.

Wang, J., Zhao, Q.H., Zhu, Z.W., Qi, L., Wang, J.X.L. and He, J.H. (2018) Interannual variation in the number and severity of autumnal haze days in the Beijing–Tianjin–Hebei region and associated atmospheric circulation anomalies. *Dynamics of Atmospheres and Oceans*, 84, 1–9.

Wang, J., Zhu, Z.W., Qi, L., Zhao, Q.H., He, J.H. and Wang, J.X.L. (2019) Two pathways of how remote SST anomalies drive the interannual variability of autumnal haze days in the Beijing–Tianjin–Hebei region, China. *Atmospheric Chemistry and Physics*, 19(3), 1521–1535.

Wang, J., Liu, Y., Ding, Y., Wu, P., Zhu, Z., Xu, Y., Li, Q., Zhang, Y., He, J., Wang, J.X.L. and Qi, L. (2020a) Impacts of climate anomalies on the interannual and interdecadal variability of autumn and winter haze in North China: a review. *International Journal of Climatology*, 40(10), 4309–4325. https://doi.org/10.1002/joc.6471.

Wang, J., Liu, Y. and Ding, Y. (2020b) On the connection between interannual variations of winter haze frequency over Beijing and different ENSO flavors. *Science of the Total Environment*, 740, 140109. https://doi.org/10.1016/j.scitotenv.2020.140109.

Wang, Y., Liu, X.N. and Ju, X.H. (2007) Differences between automatic and manual observation (in Chinese). *Journal of Applied Meteorological Science*, 18(6), 849–855.

Weng, H., Behera, S.K. and Yamagata, T. (2009) Anomalous winter climate conditions in the Pacific rim during recent El Niño Modoki and El Niño events. *Climate Dynamics*, 32(5), 663–674.

Wu, P., Ding, Y.H. and Liu, Y.J. (2017) Atmospheric circulation and dynamic mechanism for persistent haze events in the Beijing-Tianjin-Hebei region. *Advances in Atmospheric Sciences*, 34(4), 429–440.

Wu, Z. and Zhang, P. (2015) Interdecadal variability of the mega-ENSO–NAO synchronization in winter. *Climate Dynamics*, 45 (3), 1117–1128.

Xiao, D., Li, Y., Fan, S.J., Zhang, R.H., Sun, J.R. and Wang, Y. (2015) Plausible influence of Atlantic Ocean SST anomalies on winter haze in China. *Theoretical and Applied Climatology*, 122 (1), 249–257.

Xu, J.M., Chang, L.Y., Yan, F.X. and He, J.H. (2017) Role of climate anomalies on decadal variation in the occurrence of wintertime haze in the Yangtze River Delta, China. *Science of the Total Environment*, 599-600, 918–925.

Yang, Y., Liao, H. and Lou, S.J. (2016) Increase in winter haze over eastern China in recent decades: roles of variations in meteorological parameters and anthropogenic emissions. *Journal of Geophysical Research: Atmospheres*, 121(21), 13,050–13,065.

Yin, Z., Wang, H. and Chen, H. (2017) Understanding severe winter haze events in the North China plain in 2014: roles of climate anomalies. *Atmospheric Chemistry and Physics*, 17(3), 1641–1651.

Yuan, Y. and Yang, S. (2012) Impacts of different types of El Niño on the East Asian climate: focus on ENSO cycles. *Journal of Climate*, 25(21), 7702–7722.

Zhan, R., Wang, Y. and Zhao, J. (2017) Intensified mega-ENSO has increased the proportion of intense tropical cyclones over the western Northwest Pacific since the late 1970s. *Geophysical Research Letters*, 44(23), 11,959–11,966.

Zhang, P., Wang, B. and Wu, Z. (2019a) Weak El Niño and winter climate in the mid- to high latitudes of Eurasia. *Journal of Climate*, 32(2), 405–421.

Zhang, P., Wu, Z. and Chen, H. (2017) Interdecadal variability of the ENSO–North Pacific atmospheric circulation in winter. *Atmosphere-Ocean*, 55(2), 110–120.

Zhang, P., Wu, Z. and Li, J. (2019b) Reexamining the relationship of La Niña and the east Asian winter monsoon. *Climate Dynamics*, 53(1), 779–791.

Zhang, R.H., Li, Q. and Zhang, R.N. (2014) Meteorological conditions for the persistent severe fog and haze event over eastern

China in January 2013. *Science China Earth Sciences*, 57(1), 26–35.

Zhang, R. (2017) Warming boosts air pollution. *Nature Climate Change*, 7, 238–239.

Zhang, W., Wang, L., Xiang, B., Qi, L. and He, J. (2015) Impacts of two types of La Niña on the NAO during boreal winter. *Climate Dynamics*, 44(5), 1351–1366.

Zhang, Z., Sun, X. and Yang, X.-Q. (2018) Understanding the interdecadal variability of east Asian summer monsoon precipitation: joint influence of three oceanic signals. *Journal of Climate*, 31(14), 5485–5506.

Zhao, S., Li, J.P. and Sun, C. (2016) Decadal variability in the occurrence of wintertime haze in central eastern China tied to the Pacific decadal oscillation. *Scientific Reports*, 6, 27424.

Zheng, Z.F., Li, Y.X., Wang, H., Ding, H.Y., Li, Y.B., Gao, Z.Q. and Yang, Y.J. (2019) Re-evaluating the variation in trend of haze days in the urban areas of Beijing during a recent 36-year period. *Atmospheric Science Letters*, 20(1), e878.

Zhu, Z.W. and Li, T. (2016) A new paradigm for continental U.S. summer rainfall variability: Asia–North America teleconnection. *Journal of Climate*, 29(20), 7313–7327.

SUPPORTING INFORMATION

Additional supporting information may be found online in the Supporting Information section at the end of this article.